J. Phys. D: Appl. Phys. **41** (2008) 215401 (7pp) doi:10.1088/0022-3727/41/21/215401

Compositional dependence of the optical constants of amorphous $Ge_xAs_{20}Se_{80-x}$ thin films

A Dahshan[1,4], **H H Amer**[2] **and K A Aly**[3]

[1] Department of Physics, Faculty of Science, Suez Canal University, Port Said, Egypt
[2] Solid State Physics Department, National Center for Radiation Research and Technology, Atomic Energy Authority, Cairo, Egypt
[3] Physics Department, Faculty of Science, Al-Azhar University, Assiut branch, Assiut, Egypt

E-mail: adahshan73@gmail.com and kamalaly2001@gmail.com

Received 14 July 2008, in final form 9 August 2008
Published 6 October 2008
Online at stacks.iop.org/JPhysD/41/215401

Abstract

This paper reports the effect of replacement of selenium by germanium on the optical constants of chalcogenide $Ge_xAs_{20}Se_{80-x}$ (where $x = 0$, 5, 10, 15 and 20 at.%) thin films. Films of $Ge_xAs_{20}Se_{80-x}$ glasses were prepared by thermal evaporation of the bulk samples. The transmission spectra, $T(\lambda)$, of the films at normal incidence were obtained in the spectral region from 400 to 2500 nm. A straightforward analysis proposed by Swanepoel, based on the use of the maxima and minima of the interference fringes, has been applied to derive the real and imaginary parts of the complex index of refraction and also the film thickness. Increasing germanium content is found to affect the refractive index and the extinction coefficient of the $Ge_xAs_{20}Se_{80-x}$ films. Optical absorption measurements show that the fundamental absorption edge is a function of composition. With increasing germanium content the refractive index decreases while the optical band gap increases.

1. Introduction

Structural, optical and photoelectronic properties of chalcogenide amorphous thin films have been the subject of interest for many years [1–3]. This interest has been stimulated both by basic scientific questions that have to be answered in order to understand the structure and properties of these non-crystalline materials and by the need to assess their potential technological applications. Chalcogenide films have some unique properties, such as high values of refractive indices and transparency in middle and far infrared parts of the electromagnetic spectrum, that make them attractive for different applications in optoelectronics [4].

Methods for determining the optical constants of the chalcogenide amorphous thin films, based exclusively on the optical transmission spectra at normal incidence, have been made [5–8]. These relatively simple methods do not require any previous knowledge of the thickness of the films and are fairly accurate with the thickness and refractive index being determinable to within about 1% [5]. They do, however, assume that the film has a uniform thickness which, when absent, leads to less accurate results and even serious errors.

This paper is concerned with the analysis of the optical properties of as-deposited amorphous $Ge_xAs_{20}Se_{80-x}$ (where $x = 0$, 5, 10, 15 and 20 at.%) thin films, prepared by thermal evaporation. A straightforward method was proposed by Swanepoel [5], which is based on the use of maxima and minima of the interference fringes in the transmission spectrum for calculation of the refractive index and film thickness in the weakly absorbing and transparent regions of the spectrum. The absorption coefficient, and therefore the extinction coefficient, has been determined from transmission spectra in the strong absorption region. Although it is possible to find in the literature some papers dealing with both bulk and thin films [9, 10] within this composition line, to the best of our knowledge, there is no thorough study of its optical properties. Therefore, the lack of data in the literature concerning the optical characterization of films of these particular materials, along with their attractive potential technological applications, highlights the significance of the present investigation.

[4] Author to whom any correspondence should be addressed.

2. Experimental details

Different compositions of bulk $Ge_xAs_{20}Se_{80-x}$ (where $x = 0$, 5, 10, 15 and 20 at.%) chalcogenide glasses were prepared from their components of high purity (99.999%) by the melt quenching technique. The elements were heated together in an evacuated (10^{-3} Pa) silica ampoule up to 1175 K and then the ampoule temperature was kept constant for about 24 h. During the course of heating, the ampoule was shaken several times to maintain the uniformity of the melt. Finally, the ampoule was quenched into ice cooled water to avoid crystallization.

Thin films of $Ge_xAs_{20}Se_{80-x}$ were prepared by thermal evaporation of the bulk samples. The thermal evaporation process was performed inside a coating (Edward 306E) system, at a pressure of approximately 10^{-3} Pa. During the deposition process (at normal incidence), the substrates were suitably rotated in order to obtain films of uniform thickness. According to Kosa *et al* [11], the homogeneity of the studied films was clearly confirmed by the corresponding spectral dependence of transmission, where no shrinkage of the interference fringes was observed.

The elemental compositions of the investigated specimens were checked using energy dispersive x-ray (Link Analytical Edx) spectroscopy. The deviations in the elemental compositions of the evaporated thin films from their initial bulk specimens were found to be ±1.0 at.%. The amorphous state of the films was checked using an x-ray (Philips type 1710 with Cu as a target and Ni as a filter, $\lambda = 1.5418$ Å) diffractometer. The absence of crystalline peaks confirms the amorphous state of the prepared samples.

A double beam (Jasco V-630) spectrophotometer was used to measure the transmittance for the prepared films in the spectral range of wavelength from 400 to 2500 nm. Without a glass substrate in the reference beam, the measured transmittance spectra were used to calculate the optical constants of the films. In this work, the envelope method suggested by Swanepoel [5] has been applied.

3. Results and discussion

3.1. Calculation of the refractive index and film thickness

Figure 1 shows the measured transmittance, T, spectra, the created envelopes T_M and T_m and the geometric mean, $T_\alpha = \sqrt{T_M T_m}$, in the spectral region with interference fringes for the $Ge_xAs_{20}Se_{80-x}$ (where $x = 0$, 5, 10, 15 and 20 at.%) thin films, according to Swanepoel's method based on the idea of Manifacier *et al* [12]. The first approximate value of the refractive index of the film, n_1, in the spectral region of medium and weak absorption can be calculated from the following expression:

$$n_1 = \sqrt{N + \sqrt{N^2 - s^2}}, \tag{1}$$

where

$$N = 2s\frac{T_M - T_m}{T_M T_m} + \frac{s^2 + 1}{2},$$

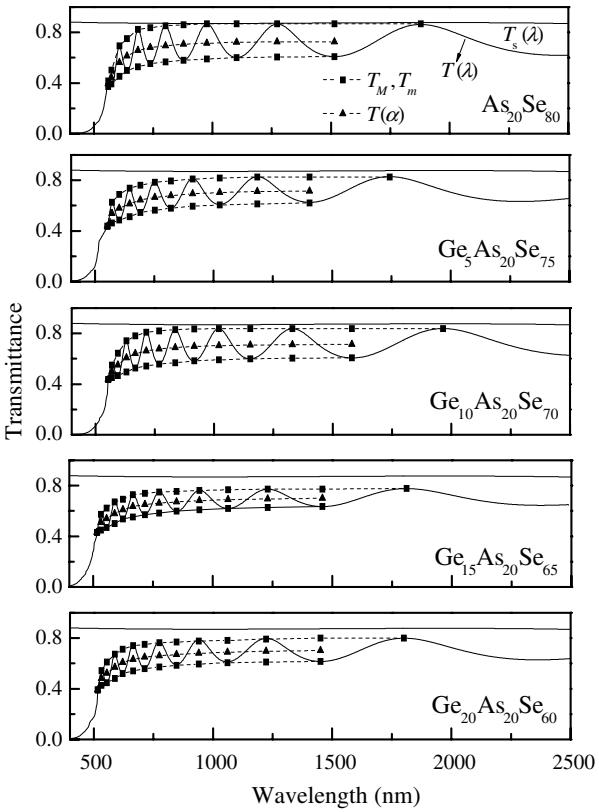

Figure 1. Transmission spectra of $Ge_xAs_{20}Se_{80-x}$ (where $x = 0$, 5, 10, 15 and 20 at.%) thin films. The average thicknesses of these samples are 723 nm, 772 nm, 708 nm, 753 nm and 789 nm for $x = 0$ at.%, 5 at.%, 10 at.%, 15 at.% and 20 at.%, respectively. Curves T_M, T_m and T_α according to the text. T_s is the transmission of the substrate alone.

where T_M and T_m are the transmission maximum and the corresponding minimum at a certain wavelength λ; alternatively, one of these values is an experimental interference maximum (minimum) and the other one is derived from the corresponding envelope. Both envelopes were computer-generated using the OriginLab (version 7) program and compared with the computer algorithm developed by McClain *et al* [13]. It is found that the two methods have the same results. The index of refraction of the substrate, s, at each wavelength is derived from the value of its transmission, $T_s(\lambda)$ [14]. The calculated values of the refractive index, n_1, using equation (1) are listed in table 1. The accuracy of this initial estimation of the refractive index is improved after calculating the thickness of the film, d, as will be explained below. Now it is necessary to take into account the basic equation for the interference fringes:

$$2nd = m_o\lambda, \tag{2}$$

where the order number, m_o, is an integer for maxima and a half-integer for minima. Moreover, if n_{c1} and n_{c2} are the refractive indices at two adjacent maxima (or minima) at λ_1 and λ_2, then the film thickness can be expressed as

$$d = \frac{\lambda_1 \cdot \lambda_2}{2(n_{c2}\lambda_1 - n_{c1} \cdot \lambda_2)}. \tag{3}$$

Table 1. Values of λ, T_s, T_M, T_m, n_1, d_1, m_o, d_2 and n_2 for $Ge_xAs_{20}Se_{80-x}$ (where $x = 0$, 5, 10, 15 and 20 at%) thin films from transmission spectra. The underlined values of transmittance are those given in the transmittance spectra of figure 1 and the others are calculated by the envelope method.

Composition	λ	s	T_M	T_m	n_1	d_1	m_o	m	d_2	n_2
$As_{20}Se_{80}$	1514	1.706	0.865	0.606	2.619		2.49	2.5	722	2.618
	1272	1.716	0.864	0.603	2.638		2.98	3	723	2.639
	1102	1.720	0.865	0.599	2.660	731	3.47	3.5	725	2.667
	976	1.722	0.865	0.587	2.707	714	3.99	4	721	2.700
	878	1.721	0.858	0.579	2.725	724	4.46	4.5	724	2.732
	802	1.717	0.850	0.564	2.769	736	4.96	5	723	2.773
	738	1.716	0.835	0.552	2.789	740	5.43	5.5	727	2.807
	686	1.713	0.820	0.525	2.877	675	6.03	6	715	2.846
	640	1.710	0.750	0.497	2.865	717	6.44	6.5	726	2.877
	$\bar{d}_1 = 719$, $\delta_1 = 22$ nm (3%); $\overline{d_2} = 723$, $\delta_1 = 3.52$ nm (0.484%)									
$Ge_5As_{20}Se_{75}$	1580	1.704	0.837	0.606	2.562		2.52	2.5	770	2.558
	1330	1.714	0.837	0.603	2.584		3.02	3	772	2.584
	1152	1.719	0.838	0.599	2.607	779	3.52	3.5	773	2.611
	1020	1.721	0.838	0.590	2.644	769	4.03	4	771	2.642
	916	1.721	0.834	0.582	2.668	768	4.53	4.5	772	2.670
	836	1.720	0.829	0.568	2.715	763	5.05	5	769	2.707
	768	1.717	0.819	0.558	2.735	772	5.53	5.5	772	2.736
	714	1.715	0.809	0.541	2.786	763	6.06	6	768	2.775
	668	1.712	0.780	0.525	2.796	799	6.51	6.5	776	2.812
	630	1.709	0.740	0.495	2.852	799	7.04	7	773	2.856
	$\bar{d}_1 = 777$, $\delta_1 = 15$ nm (2.1%); $\overline{d_2} = 772$, $\delta_1 = 2.27$ nm (0.29%)									
$Ge_{10}As_{20}Se_{70}$	1404	1.711	0.824	0.618	2.495		2.49	2.5	703	2.479
	1184	1.719	0.823	0.611	2.528		3.00	3	702	2.508
	1026	1.721	0.815	0.603	2.538	717	3.48	3.5	707	2.536
	912	1.721	0.808	0.593	2.558	746	3.94	4	713	2.576
	820	1.719	0.792	0.578	2.590	730	4.44	4.5	712	2.606
	752	1.717	0.783	0.561	2.641	707	4.94	5	711	2.655
	692	1.713	0.759	0.545	2.657	733	5.39	5.5	716	2.688
	646	1.710	0.735	0.51	2.775	638	6.04	6	698	2.737
	602	1.707	0.687	0.484	2.774	650	6.48	6.5	705	2.763
	$\bar{d}_1 = 703$, $\delta_1 = 42$ nm (6.0%); $\overline{d_2} = 708$, $\delta_1 = 5.94$ nm (0.84%)									
$Ge_{15}As_{20}Se_{65}$	1450	1.709	0.797	0.614	2.447		2.56	2.5	740	2.407
	1222	1.717	0.789	0.609	2.456		3.04	3	746	2.434
	1060	1.721	0.780	0.604	2.458	791	3.51	3.5	754	2.463
	940	1.721	0.775	0.594	2.488	784	4.01	4	755	2.497
	846	1.720	0.767	0.584	2.509	773	4.49	4.5	758	2.528
	774	1.718	0.761	0.571	2.549	774	4.99	5	759	2.570
	712	1.715	0.749	0.558	2.575	767	5.48	5.5	760	2.600
	664	1.712	0.738	0.538	2.639	734	6.02	6	754	2.645
	620	1.708	0.710	0.518	2.660	741	6.49	6.5	757	2.676
	588	1.706	0.670	0.480	2.750	711	7.08	7	748	2.733
	554	1.702	0.608	0.446	2.753	737	7.52	7.5	754	2.759
	$\bar{d}_1 = 757$, $\delta_1 = 27$ nm (3.6%); $\overline{d_2} = 753$, $\delta_1 = 6.13$ nm (0.81%)									
$Ge_{20}As_{20}Se_{60}$	1458	1.709	0.773	0.634	2.304		2.47	2.5	791	2.310
	1230	1.717	0.771	0.626	2.340		2.97	3	788	2.338
	1064	1.721	0.767	0.619	2.361	782	3.47	3.5	788	2.360
	944	1.721	0.762	0.608	2.395	787	3.96	4	788	2.393
	848	1.720	0.755	0.598	2.418	791	4.45	4.5	789	2.418
	776	1.718	0.749	0.584	2.461	788	4.95	5	788	2.459
	716	1.715	0.738	0.571	2.487	803	5.42	5.5	791	2.496
	666	1.712	0.727	0.553	2.537	782	5.95	6	787	2.532
	624	1.709	0.693	0.535	2.525	872	6.32	6.5	803	2.570
	590	1.706	0.671	0.499	2.646	741	7.00	7	780	2.617
	556	1.703	0.622	0.469	2.657	682	7.46	7.5	784	2.643
	$\bar{d}_1 = 781$, $\delta_1 = 50$ nm (6.4%); $\overline{d_2} = 789$, $\delta_1 = 5.64$ nm (0.72%)									

The values of d determined by this equation for different samples are listed as d_1 in table 1. The last value deviates considerably from the other values and must consequently be rejected. The average value, $\overline{d_1}$, of d_1 (ignoring the last value), can now be used, along with n_1 to calculate m_o for the different maxima and minima using equation (2). The accuracy of the film thickness can now be significantly increased by taking the corresponding exact integer or half-integer values of m_o

associated with each extreme point (see figure 1) and deriving a new thickness, d_2. The values of the thickness in this way have a smaller dispersion. It should be emphasized that the accuracy of the final thickness is better than 1% (see table 1).

With the accurate values of m_o and the average value $\overline{d_2}$ of d_2, expression (2) can then be solved for n at each λ and, thus, the final values of the refractive index, n_2, are obtained. These values are listed in table 1.

Figure 2 illustrates the dependence of the refractive index, n, on the wavelength for different compositions of the amorphous $Ge_xAs_{20}Se_{80-x}$ (where $x = 0$, 5, 10, 15 and 20 at.%) thin films. Now the values of n_2 can be fitted to a function such as the two-term Cauchy dispersion relationship [15]:

$$n(\lambda) = a + \frac{b}{\lambda^2}, \tag{4}$$

which can then be used to extrapolate the wavelength dependence beyond the range of measurement (see figure 2). This figure shows that the refractive index decreases with increasing Ge content over the entire spectral range studied. The least-squares fit of n_2 for the different samples listed in table 1 yields $n = 2.56 + (1.37 \times 10^5/\lambda^2)$, $n = 2.51 + (1.38 \times 10^5/\lambda^2)$, $n = 2.416 + (1.30 \times 10^5/\lambda^2)$, $n = 2.346 + (1.28 \times 10^5/\lambda^2)$ and $n = 2.253 + (1.23 \times 10^5/\lambda^2)$ for $x = 0$ at.%, 5 at.%, 10 at.%, 15 at.% and 20 at.%, respectively.

The final values of the refractive index can be fitted to an appropriate function such as the Wemple–DiDomenico (WDD) dispersion relationship [16], i.e. to the single-oscillator model:

$$n^2(h\nu) = 1 + \frac{E_o E_d}{E_o^2 - (h\nu)^2}, \tag{5}$$

where E_o is the single-oscillator energy and E_d is the dispersion energy or single-oscillator strength. By plotting $(n^2-1)^{-1}$ against $(h\nu)^2$ and fitting straight lines as shown in figure 3, E_o and E_d can be determined from the intercept, E_o/E_d, and the slope, $(E_o E_d)^{-1}$. The oscillator energy, E_o, is an average energy gap and to a good approximation scales with the optical band gap, $E_o \approx 2E_g$, as was found by Tanaka [17]. Figure 3 also shows the values of the refractive index $n(0)$ at $h\nu = 0$ for the $Ge_xAs_{20}Se_{80-x}$ (where $x = 0$, 5, 10, 15 and 20 at.%) films. The obtained values of E_o, E_d and $n(0)$ are listed in table 2. It was observed that the single oscillator energy, E_o, increases while the dispersion energy, E_d, and the refractive index $n(0)$ decrease with increasing Ge content.

The dependence of the refractive index on the lattice dielectric constant, ε_L, is given by [18]:

$$n^2 = \varepsilon_L - (e^2/\pi c^2)(N/m^*)\lambda^2, \tag{6}$$

where N/m^* is the ratio of the carrier concentration, N, to the effective mass, m^*, c is the speed of light and e is the electronic charge. The plots of n^2 versus λ^2 for the $Ge_xAs_{20}Se_{80-x}$ (where $x = 0$, 5, 10, 15 and 20 at.%) thin films as shown in figure 4 are linear, verifying equation (6). The values of ε_L and N/m^* were deduced from the extrapolation of these plots to $\lambda^2 = 0$ and from the slope of the graph, respectively. The obtained values for ε_L and N/m^* for the $Ge_xAs_{20}Se_{80-x}$ (where $x = 0$, 5, 10, 15 and 20 at.%) thin films are listed in table 2.

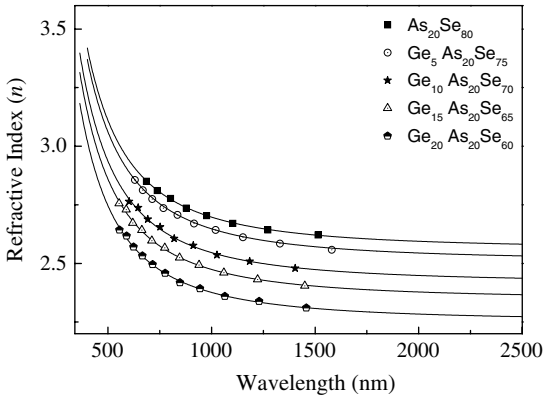

Figure 2. Refractive index dispersion spectra for $Ge_xAs_{20}Se_{80-x}$ (where $x = 0$, 5, 10, 15 and 20 at.%) thin films. Solid curves are determined according to the Cauchy dispersion relationship [15].

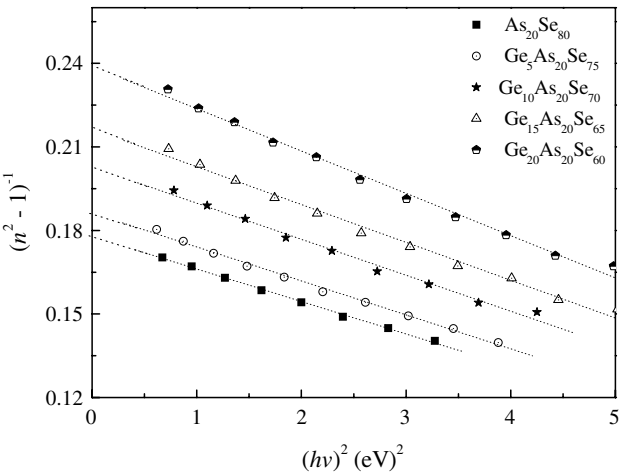

Figure 3. Plots of refractive index factor $(n^2 - 1)^{-1}$ versus $(h\nu)^2$ for $Ge_xAs_{20}Se_{80-x}$ (where $x = 0$, 5, 10, 15 and 20 at.%) thin films.

The decrease in the refractive index, n, and in the dispersion energy, E_d, with increasing Ge content could be explained by the decrease in the carrier concentration, N [19], as shown in table 2.

Furthermore, a simple complementary graphical method for deriving the first-order number, m_1, and film thickness, d, based on equation (2) was also used. For this purpose equation (2) can now be written for the extremes of the spectrum as [2]

$$\frac{l}{2} = 2d \cdot \left(\frac{n}{\lambda}\right) - m_1, \tag{7}$$

where $l = 0$, 1, 2, 3, ... for the successive tangent points, starting from the long wavelength end, and m_1 is the order number of the first ($l = 0$) tangent point considered. Therefore, by plotting $(l/2)$ versus (n/λ) we obtain a straight line with the slope $2d$ and the cut-off on the vertical axis at $-m_1$ as shown in figure 5. The obtained values of $2d$ and m_1 for the $Ge_xAs_{20}Se_{80-x}$ (where $x = 0$, 5, 10, 15 and 20 at.%) thin films are displayed as shown in this figure.

Table 2. Some physical parameters as a function of Ge content for $Ge_xAs_{20}Se_{80-x}$ (where $x = 0$, 5, 10, 15 and 20 at.%) specimens.

Composition	E_g (eV)	E_o (eV)	E_d (eV)	E_o/E_g	$n(0)$	$N/m*$ (10^{43} m^3)	ε_L	Excess of Se–Se bonds	CE (eV atom^{-1})
$As_{20}Se_{80}$	1.84	3.851	21.64	2.098	2.57	5.00	6.93	100	2.037
$Ge_5As_{20}Se_{75}$	1.88	3.905	20.99	2.072	2.53	4.91	6.67	70	2.179
$Ge_{10}As_{20}Se_{70}$	1.91	3.967	19.54	2.073	2.43	4.47	6.17	40	2.321
$Ge_{15}As_{20}Se_{65}$	1.97	4.010	18.59	2.042	2.37	4.28	5.82	10	2.463
$Ge_{20}As_{20}Se_{60}$	2.02	4.041	17.00	1.995	2.28	3.95	5.37	—	2.53

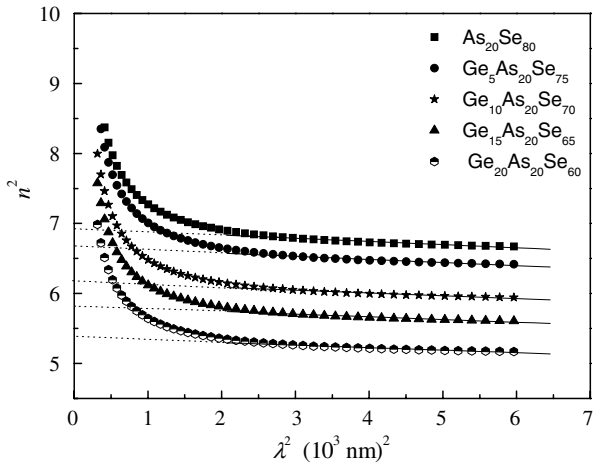

Figure 4. Plots of n^2 versus λ^2 for $Ge_xAs_{20}Se_{80-x}$ (where $x = 0$, 5, 10, 15 and 20 at.%) thin films.

3.2. Determination of the extinction coefficient and optical band gap

Continuing with the description of the data processing method, when there is no substrate in the reference beam and the values of the refractive index and the thickness of the films are already known, the absorption coefficient, α, is derived using the interference-free transmission spectrum, T_α (see figure 1), over the whole spectral range, using the well-known equation suggested by Connell and Lewis [20]:

$$\alpha = -\frac{1}{d}\ln\left(\frac{1}{B}\left\{A + [A^2 + 2BT_\alpha(1 - R_2R_3)]^{1/2}\right\}\right), \quad (8)$$

where $A = (R_1 - 1)(R_2 - 1)(R_3 - 1)$, $B = 2T_\alpha(R_1R_2 + R_1R_3 - 2R_1R_2R_3)$, R_1 is the reflectance of the air–film interface ($R_1 = [(1 - n)/(1 + n)]^2$), R_2 is the reflectance of the film–substrate interface ($R_2 = [(n - s)/(n + s)]^2$) and R_3 is the reflectance of the substrate–air interface ($R_3 = [(s - l)/(s + 1)]^2$). To complete the calculations of the optical constants, the extinction coefficient, k, is calculated using the values of α and λ by the well-known relation $k = \alpha\lambda/4\pi$. Figure 6 illustrates the dependence of k on the photon energy for $Ge_xAs_{20}Se_{80-x}$ (where $x = 0$, 5, 10, 15 and 20 at.%) thin films. For $\alpha \leqslant 10^5$ cm^{-1}, the imaginary part of the complex index of refraction is much less than n, so that the previous expressions used to calculate the reflectance are valid. In the region of strong absorption, the interference fringes disappear; in other words, for very large α the three curves T_M, T_α and T_m converge to a single curve.

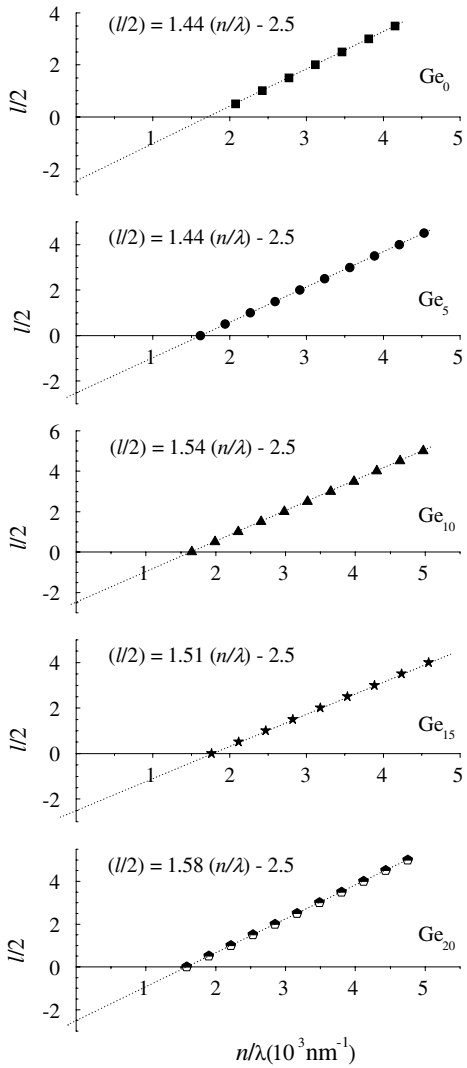

Figure 5. Plots of (l/2) versus (n/λ) to determine the film thickness and the first-order number, m_1, for $Ge_xAs_{20}Se_{80-x}$ (where $x = 0$, 5, 10, 15 and 20 at.%) thin films.

According to Tauc's relation [21, 22] for allowed non-direct transitions, the photon energy dependence of the absorption coefficient can be described by

$$(\alpha h\nu)^{1/2} = B(h\nu - E_g), \quad (9)$$

where B is a parameter that depends on the transition probability and E_g is the optical energy gap. Figure 7 shows the absorption coefficient in the form of $(\alpha h\nu)^{1/2}$ versus $h\nu$ for the $Ge_xAs_{20}Se_{80-x}$ (where $x = 0$, 5, 10, 15 and 20 at.%) films.

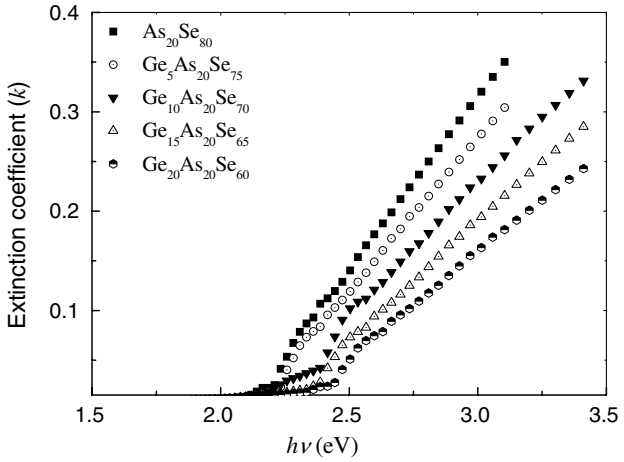

Figure 6. Extinction coefficient, k, versus $h\nu$ for $Ge_xAs_{20}Se_{80-x}$ (where $x = 0$, 5, 10, 15 and 20 at.%) thin films.

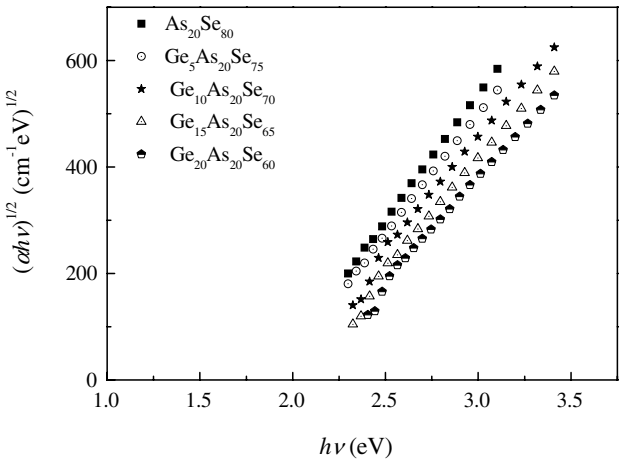

Figure 7. Dependence of $(\alpha h\nu)^{1/2}$ on photon energy, $h\nu$, for $Ge_xAs_{20}Se_{80-x}$ (where $x = 0$, 5, 10, 15 and 20 at.%) thin films from which the optical band gap, E_g, is estimated (Tauc extrapolation).

The intercepts of the straight lines with the photon energy axis yield the values of the optical band gap. The variation of E_g as a function of the Ge content for the thin films is depicted in figure 8.

From this figure, it is clear that E_g increases with increasing Ge content for the investigated films. This behaviour is in good agreement with many authors [23–25]. They found that the optical band gap increases with increasing Ge content in the As–Ge–Se and Ge–Se systems. The increase in the optical band gap with increasing Ge content can be interpreted on the basis of the chemical-bond approach proposed by Bicerano and Ovshinsky [26].

Knowing the bond energies of the various bonds involved in the Ge–As–Se system [2], we can estimate the cohesive energy, CE, i.e. the stabilization energy of an infinitely large cluster of the material per atom, by summing the bond energies over all the bonds expected in the system under test. The CE of the prepared samples is evaluated from the following equation $\mathrm{CE} = \sum(C_i D_i/100)$, where C_i and D_i are the numbers of the expected chemical bonds and the energy of each corresponding bond, respectively [27]. The calculated

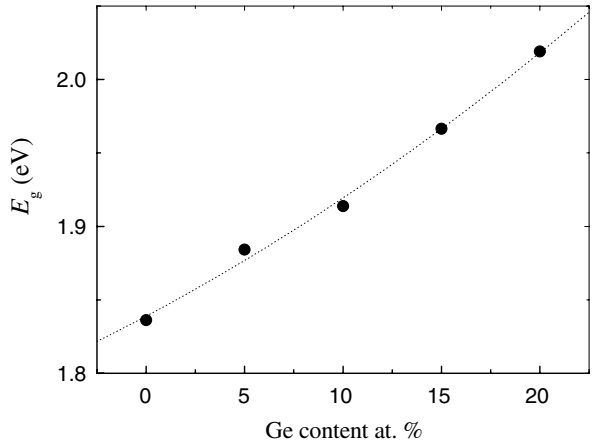

Figure 8. Variation in the optical band gap, E_g, as a function of Ge content for $Ge_xAs_{20}Se_{80-x}$ (where $x = 0$, 5, 10, 15 and 20 at.%) thin films.

values of the CE for all compositions are presented in table 2. It is observed that the CE increases with increasing Ge content. The increase in the CE with increasing Ge content is due to the decrease in the excess of Se–Se homopolar bonds (see table 2). This result is in good agreement with many authors [2, 28, 29].

The bond energies of the bonds involving, namely, Ge–Se, As–Se and Se–Se are, respectively, equal to 49.44 kcal mol^{-1}, 41.71 kcal mol^{-1} and 44.04 kcal mol^{-1} [2]. For the Ge–As–Se system, Ge and As atoms bond to Se atoms to form $GeSe_2$ and As_2Se_3 structural units, respectively. After forming Ge–Se and As–Se bonds there are still unsatisfied Se valences which must be satisfied by the formation of Se–Se bonds (Se chains). With increasing Ge content the $GeSe_2$/Se ratio progressively increases. The optical gap could be obtained from the addition of the partial optical gaps of the different structural phases formed inside the film. With increasing Ge content, the $GeSe_2$ ($E_g = 2.2$ eV [30]) phase replaces the Se ($E_g = 1.95$ eV [2]) phase which is behind the increase in the optical gap of the films with increasing Ge content.

The increase in the optical band gap, i.e. the increase in the network order, is accompanied by a decrease in polarizability, which leads to the decrease in the refractive index, n, and in the dispersion energy, E_d, with increasing Ge content [31].

4. Conclusions

Optical data indicated that the allowed non-direct gap is responsible for the photon absorption in the $Ge_xAs_{20}Se_{80-x}$ thin films. The optical band gap has been determined from the spectral dependence of the absorption coefficient using the Tauc formula. It was found that the optical band gap, E_g, and the single-oscillator energy, E_o, increase, while the refractive index, n, and the dispersion energy, E_d, decrease with increasing Ge content in the films. The dispersion of the refractive index is discussed in terms of the single-oscillator WDD model. The chemical-bond approach can be applied successfully to interpret the increase in the optical gap with increasing Ge content.

References

[1] Marquez E, Gonzalez-Leal J M, Jimenez-Garay R and Vlcek M 2001 *Thin Solid Films* **396** 183
[2] Dahshan A and Aly K A 2008 *Phil. Mag.* **88** 361
[3] Dahshan A, Amer H H, Moharram A H and Othman A A 2006 *Thin Solid Films* **513** 369
[4] Zakery A and Elliott S R 2003 *J. Non-Cryst. Solids* **330** 1
[5] Swanepoel R 1983 *J. Phys. E: Sci. Instrum.* **16** 1214
[6] Swanepoel R 1984 *J. Phys. E: Sci. Instrum.* **17** 896
[7] Dahshan A and Aly K A 2008 *Acta Mater.* **56** 4869
[8] Aly K A, Dahshan A and Abousehly A M 2008 *Phil. Mag.* **88** 47
[9] Mammadov E and Taylor P C 2008 *J. Non-Cryst. Solids* **354** 2732
[10] El-Nahass M M, El-Deeb A F, El-Sayed H E A and Hassanien A M 2006 *Opt. Laser Technol.* **38** 146
[11] Kosa T I, Wagner T, Ewen P J S and Owen A E 1995 *Phil. Mag.* B **71** 311
[12] Manifacier J C, Gasiot J and Fillard J P 1976 *J. Phys. E: Sci. Instrum.* **9** 1002
[13] McClain M, Feldman A, Kahaner D and Ying X 1991 *J. Comput. Phys.* **5** 45
[14] Jenkins F A and White H E 1957 *Fundamentals of Optics* (New York: McGraw-Hill)
[15] Moss T S 1959 *Optical Properties of Semiconductors* (London: Buttenworths)
[16] Wemple S H and DiDomenico M 1971 *Phys. Rev.* B **3** 1338
[17] Tanaka K 1980 *Thin Solid Films* **66** 271
[18] Kumar G, Thomas J, George N, Kumar B, Shnan P, Npoori V, Vallabhan C and Unnikrishnan N 2001 *Phys. Chem. Glasses* **41** 89
[19] Abdel-Aziz M M, El-Metwally E G, Fadel M, Labib H H and Afifi M A 2001 *Thin Solid Films* **386** 99
[20] Connell G A N and Lewis A J 1973 *Phys. Status Solidi* b **60** 291
[21] Fritzsche H 1993 *Phil. Mag.* B **68** 561
[22] Davis E A and Mott N F 1970 *Phil. Mag.* **22** 903
[23] Afaf A Abd El-Rahman, Eid A M, Sanad M and El-Ocker R M 1998 *J. Phys. Chem. Solids* **59** 825
[24] Nagels P, Tichy L, Sleeckx E and Callaerts R 1998 *J. Non-Cryst. Solids* **227–230** 705
[25] Tichy L, Ticha H, Nagels P and Callaerts R 1998 *J. Non-Cryst. Solids* **240** 177
[26] Bicerano J and Ovshinsky S R 1985 *J. Non-Cryst. Solids* **74** 75
[27] Fayek S A 2001 *J. Phys. Chem. Solids* **62** 653
[28] Fayek S A, El-Ocker M and Hassanien A S 2001 *Mater. Chem. Phys.* **70** 231
[29] Fouad S S, Bekheet A E and Farid A M 2002 *Physica* B **322** 163
[30] Sakai K, Maeda K, Yokoyama H and Ikari T 2003 *J. Non-Cryst. Solids* **320** 223
[31] Munzar M, Tichy L and Ticha H 2002 *Curr. Appl. Phys.* **2** 181